Journal of Alloys and Compounds 739 (2018) 600–606

Contents lists available at ScienceDirect

Journal of Alloys and Compounds

journal homepage: http://www.elsevier.com/locate/jalcom

Dielectric and Magnetic Properties of $Ni_xPb_{1-x}TiO_3$ Solid Solution and Composite: Coexistence of Ferroelectric and Antiferromagnetic Order

R.C. da Costa [a, b], J.E. Rodrigues [b, c, *], A.J. Gualdi [b], T.R. Cunha [b, *], A.D. Rodrigues [b], P.W. Marques [b], A.C. Hernandes [c], P.S. Pizani [b]

[a] Universidade Federal de Campina Grande, Centro de Ciências & Tecnologia Agroalimentar, 58840-000, Pombal, PB, Brazil
[b] Universidade Federal de São Carlos, Departamento de Física, C.P.676, 13565-905, São Carlos, SP, Brazil
[c] Instituto de Física de São Carlos, Universidade de São Paulo, 13560-970, São Carlos, SP, Brazil

ARTICLE INFO

Article history:
Received 25 September 2017
Received in revised form
11 November 2017
Accepted 23 December 2017
Available online 28 December 2017

Keywords:
$Ni_xPb_{1-x}TiO_3$
Composite
Ferroelectric order
Antiferromagnetic order
Magnetoelectric

ABSTRACT

A complete serie of $Ni_xPb_{1-x}TiO_3$ samples were synthesized by solid state reaction and their structural, vibrational, dielectric and magnetic properties were properly characterized using X-ray diffraction, Raman scattering, dielectric permittivity, magnetic susceptibility and magnetization loops. The XRD and Raman results showed the formation of solid solutions for *x* below 0.3, while for higher values of *x* there is preferentially the formation of a $PbTiO_3$ and $NiTiO_3$ composite. The dielectric and magnetic measurements exhibited the coexistence of the ferroelectric and antiferromagnetic orders for Ni concentrations from 0.3 to 0.9, a very interesting result for magnetoelectric device application.

© 2017 Elsevier B.V. All rights reserved.

1. Introduction

During the last decades, materials with simple or complex perovskite structure have been widely investigated because their physicochemical properties, which permits a very large variety of technological applications in sensors, actuators, dielectric resonators, capacitors [1] [2]. In the group of simple perovskites, those with ABO_3 structure stand out by the possibility of presenting ferroelectric order. These materials are very interesting because the *A* and/or *B* sites can be occupied by a vast number of elements, including transition metals, which leads to distinguished properties. More recently, it was opened up the possibility to generate magnetoelectric properties by incorporating magnetic ions, which points to potential application in new devices controlled by the both magnetic and electric fields [3] [4] [5].

In fact, atomic substitution is an effective route for the development of materials with new structural characteristics [6], especially when the substituting ion presents very different crystal radius. In that case, the use of low concentrations of substituting ion results in solid solutions, while high concentrations induce the formation of composites. Another possibility to control the final structural characteristics can be found in compounds in which the extremes of the compositional range present different crystallographic structures. The system $Ni_xPb_{1-x}TiO_3$ (hereafter NPT) system meets these two conditions. Firstly because in these compounds the crystal radii of Pb^{2+} is 1.63 Å, while Ni^{2+} is only 0.83 Å. Secondly, since $PbTiO_3$ (PT) is a ferroelectric ABO_3 perovskite with tetragonal symmetry at room conditions, while $NiTiO_3$ (NT) is also ABO_3-type, but with rhombohedral ilmenite symmetry. Additionally, nickel titanate presents antiferromagnetic order below 23 K, which makes NPT particularly interesting.

In this paper will be presented a study of the dielectric and magnetic properties of NPT for all compositions in a range varying from PT to NT. The results are confronted with Raman spectroscopy and X-ray diffraction [7], that are complementary techniques, since it is possible to establish a strong correlation between the wavenumber of PT-like E(1TO) soft mode and the unit cell volume. Also, differential scanning calorimetry will be presented viewing to corroborate the analyses of modifications in Curie temperature, in which the ferroelectric to paraelectric transition occurs.

* Corresponding authors. Universidade Federal de São Carlos, Departamento de Física, C.P.676, 13565-905, São Carlos, SP, Brazil.
E-mail addresses: rodrigues.joaoelias@gmail.com, rodrigues.joaoelias@df.ufscar.br (J.E. Rodrigues), thiago@df.ufscar.br (T.R. Cunha).

https://doi.org/10.1016/j.jallcom.2017.12.273
0925-8388/© 2017 Elsevier B.V. All rights reserved.

2. Experimental procedures

$Ni_xPb_{1-x}TiO_3$ samples were synthesized by solid state reaction method with compositions in the interval $0.0 \leq x \leq 1.0$ with an increment of 0.10. The stoichiometries were controlled by milling different proportions of precursor oxides PbO, NiO and TiO_2 (Sigma-Aldrich purity > 99%) in a high energy vibratory mill during 1 h. Then, the mixtures were calcined for 1 h at different temperatures depending on composition, with values varying from 975 K, for PbO + TiO_2, up to 1375 K for NiO + TiO_2. The stoichiometry of each sample was confirmed by EDX analysis. Details can be found in Ref. [7].

XRD measurements were performed at room conditions in the range from 20° to 80° with a Shimadzu diffractometer model 6100 using accelerating voltage of 40 kV with Cu-Kα radiation (λ = 1.5406 Å). By means of Rietveld refinements, accomplished with free software GSAS [8] [9], lattice parameters and unit cell volumes of PT phase were calculated for of all $Ni_xPb_{1-x}TiO_3$ samples. Details on the quantification of crystalline phases can be found in Fig. S1 of Supplementary Data. Raman scattering was measured with a HR800 Evolution micro-Raman spectrometer by Horiba-*Jobin-Yvon*, using the 532 nm line of the Nd-YAG laser as excitation source. For the high temperature measurements, samples were set in a Linkan TS1500 micro furnace. Raman scattering is a powerful technique used in the study of these systems, mainly because the PT-like Raman mode with lowest wavenumber E(1TO), called soft mode, is very sensitive even to slight changes in the symmetry, serving as a probe for structural modifications [10]. All spectra were divided by the Bose-Einstein thermal factor $[n(\omega,T) + 1]$ [11]. The Curie temperature of the $Ni_xPb_{1-x}TiO_3$ was determined by differential scanning calorimetry (DSC) in a Netzsch DSC 200 F3 Maia, at a heating rate of 10 K min^{-1} from 298 K to 873 K, under argon atmosphere and sample weight of 16 mg for each composition.

To study the dielectric properties of $Ni_xPb_{1-x}TiO_3$ ceramics, metallic parallel surfaces were prepared after a polishing process and a platinum deposition. A sinusoidal electric field (*ac* voltage ~ 1 V) was applied to the parallel plate capacitor, being the output signal collected by a frequency response analyzer (Solartron 1260 coupled with a dielectric interface Solartron 1296A). To obtain the complex permittivity ($\varepsilon^* = \varepsilon' + j\varepsilon''$) spectra between 1 Hz and 1 MHz, the electrical impedance [$Z^* \sim (j\omega\varepsilon^*)^{-1}$] spectra were collected in a temperature scanning mode by using a homemade tubular furnace, upon cooling (298–823 K; 2 K min^{-1}). The room temperature impedance spectra of all samples depicted two contributions ascribed to the grain boundaries (at low frequency) and grain (or bulk, at high frequency) [12] [13]. For this reason, we analyzed only the high frequency data in this paper, only concerning the bulk (grain) features.

Magnetic measurements were performed in a Quantum Design MPMS3 SQUID magnetometer. In the zero field cooling (ZFC) measurements, the samples were cooled down, from 300 K to 5 K, without magnetic field. After reach 5 K, the magnetization was measured during the temperature increasing from 5 K to 300 K with an applied magnetic field of 50 Oe. In the field cooled cooling (FCC) measurements, the magnetization was measured during the temperature cooled down to 5 K with magnetic field of same intensity. The M × H magnetization loops were performed at 300 K and magnetic field up to 70 kOe.

3. Results and discussion

3.1. X-Ray diffraction, Raman scattering and differential scanning calorimetry

Viewing the completeness of the discussions, a part of some results already published in Ref. [7] will be briefly presented. Raman and XRD studies performed in our samples showed that the existence of two resulting nickel lead titanate products have to be considered, see details in Fig. S1 of Supplementary Data, depending on the relative concentration of Ni and Pb. For low Ni concentrations ($x < 0.3$) there is a majority formation of a solid solution in which Pb is substituted by Ni, whereas for higher Ni proportions there is also the formation of $Ni_xPb_{1-x}TiO_3$ and a composite with $PbTiO_3$ perovskite and $NiTiO_3$ ilmenite phases (details in Ref. [7]).

Fig. 1 depicts the soft mode wavenumbers and unit cell volumes of PT phase, as a function of Ni concentration. For low Ni concentrations up to ~ 0.4 both parameters decrease as a consequence of lattice distortions induced by the atomic substitution of Pb for Ni. For concentrations above 0.4 they are only partially recovered until x ~ 0.8, although the initial value is not restored even for very low Pb concentrations, indicating hence the formation of a composite in the high Ni concentration range.

Fig. 2 (a) displays the DSC curves of the $Ni_xPb_{1-x}TiO_3$ system. For a better comprehension only the data of odd proportions of Ni are exhibited. The endothermic peaks on heating characterize the Curie temperature related to tetragonal-ferroelectric to cubic-paraelectric transition of PT phases T_C [14], whose values are shown in Fig. 2 (b), from which can be noticed that the substitution of Ni for Pb induces a decrease of T_C in samples with $x \leq 0.5$ Ni, reaching the minimum of 721 K for the concentration with 0.5 Ni. For x higher than 0.5, T_C increases and remains nearly constant for $x > 0.7$. The broadening of the peaks, measured by the difference between the onset and the ending temperatures ΔT, also depends on the Ni concentration. In Fig. 2 (c), it is shown that ΔT significantly increases in the solid solution region (from 0.0 to ~ 0.4) and that the endothermic peak narrows again above this concentrations, defining a maximum of ΔT profile at intermediate concentrations, where structural and chemical disorders induced by the substitution of Ni by Pb are maxima. The decrease of ΔT accompanied by the increasing in T_C for $x \geq 0.5$ Ni is a consequence of the fact that we preferentially have a composite in this region.

Fig. 3 exhibits the *in situ* Raman spectra for all Ni contents at temperatures above their corresponding Curie temperature. In cubic-paraelectric phase all the vibrational modes are not active in the Raman scattering, since $\Gamma_{Vibrational} = 3F_{1u}$ for the *Pm*-3*m* simple cubic unit cell. In Fig. 3 (a), the Raman spectra for $x < 0.3$ shows only broad bands with very low intensity similar to pure PT in cubic phase, with no characteristic peaks of NT phase. On the other hand, for $x > 0.3$, the spectra present only the Raman peaks of NT, see

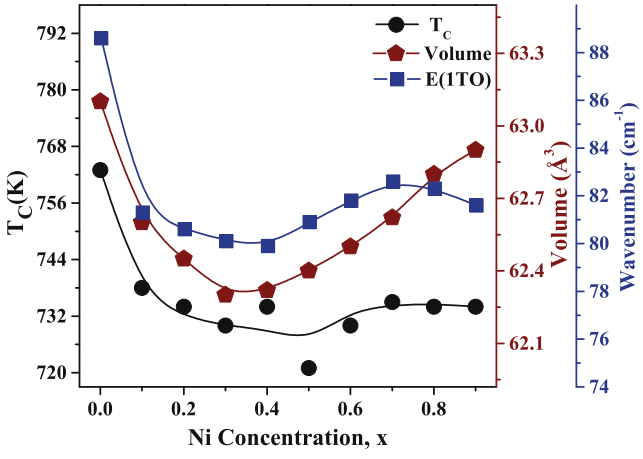

Fig. 1. Dependence of PT-like soft mode wavenumber, unit cell volume and Curie temperature (T_C) obtained from Raman scattering as a function of Ni concentration.

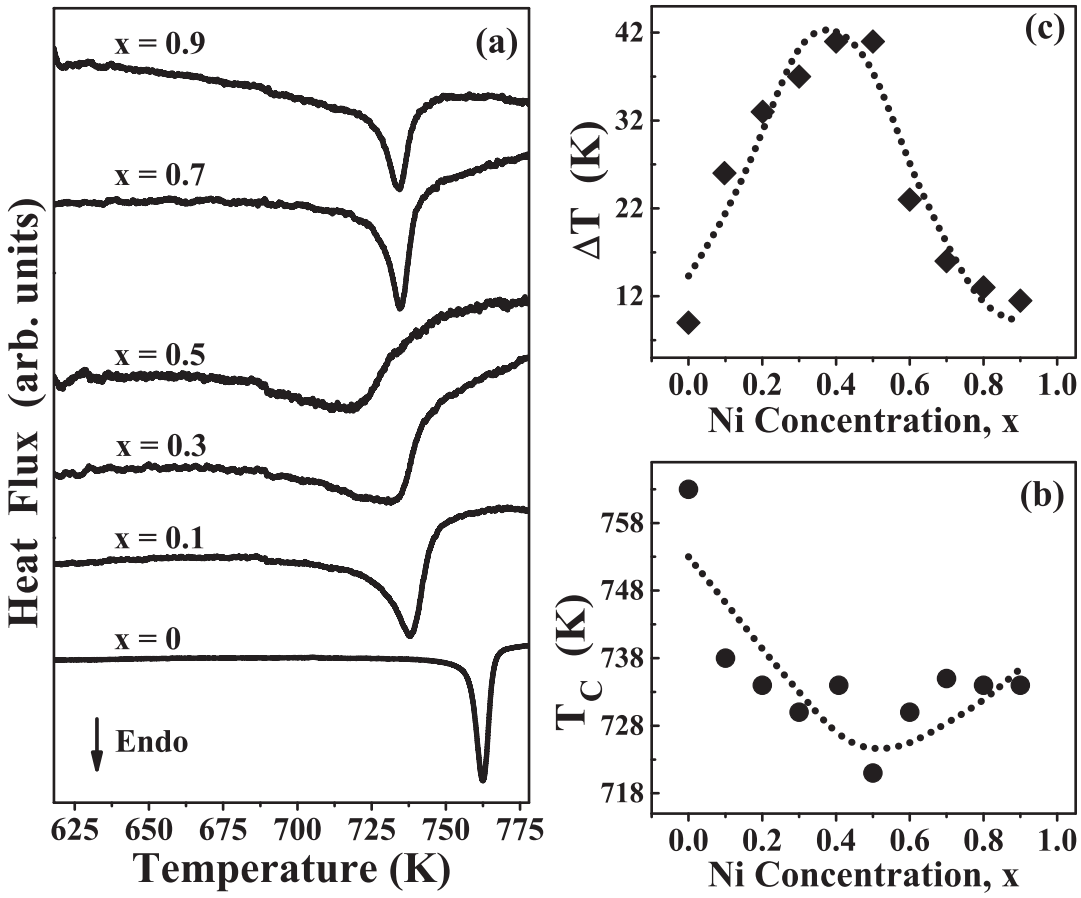

Fig. 2. (a) DSC curves of $Ni_xPb_{1-x}TiO_3$ through which (b) the T_C Curie temperatures and (c) the broadening of the endothermic peaks were determined. Dashed lines are guides to the eyes.

details in Fig. 3 (b), corroborating our previous observation that for higher *x* values, there is a preferential formation of a composite.

3.2. Dielectric properties

The temperature dependence of the real part (ε') of the dielectric permittivity of $Ni_xPb_{1-x}TiO_3$ ceramics and their dielectric loss (tan δ) are exhibited in Fig. 4, particularly for $x = 0.00$ (a); 0.20 (b); 0.70 (c) and 1.00 (d). The measurements were performed at selected frequencies (10 kHz, 100 kHz and 1 MHz) and upon cooling. As one can note, samples containing lead in their compositions present an abrupt increase in ε', being this phenomenon related to the paraelectric (PE) → ferroelectric (FE) transition [15]. This transition is not expected in the $NiTiO_3$ sample, since it belongs to the ilmenite family with a rhombohedral space group $-R$-3:H (C_{3i}^2 or #148) [16]. In Fig. 4 (d), it can only be observed a well-defined plateau behavior. From the insets of Fig. 4 (a-b), we can additionally conclude that the PE → FE transition temperature is independent of the frequency, which denotes that the lead containing samples keep themselves as normal ferroelectrics, (i.e. relaxor state was not found in our compositions). Such behavior was also detected for the samples with intermediate *x* values, from 0.0 to 0.9, not shown.

Fig. 5 (a-b) illustrates the ε' vs. temperature curve measured at 1 MHz for the $Ni_xPb_{1-x}TiO_3$ ceramics. It is clearly noticed that the PE → FE transition temperature depends on the nickel content. As expected, the transition temperatures derived from both ε' and tan δ curves are similar, see insets in Fig. 5 (a-b). Fig. 5 (c) depicts the Ni content dependence of the PE → FE transition temperature T_C calculated from Fig. 5 (a-b). The decreasing of T_C until $x \sim 0.4$, followed by a recovering, is attributed to the formation of solid solutions in this composition interval [7], where Ni cations partially occupy the original sites of Pb in ferroelectric tetragonal unit cell. Otherwise, it was detected a composite behavior for the $Ni_xPb_{1-x}TiO_3$ ceramics with $x > 0.4$. A piece of evidence for this fact comes from the Ni content dependence of the real permittivity ε' at room temperature in Fig. 5 (d). For $x \geq 0.4$, the ε' value decreases monotonically until about 20 ($x = 1.00$; $\varepsilon'_{NT} = 20$ at 1 MHz). This fact can be explained in light of the Lichtenecker mixture rule, defined as follows [17]:

$$\log \varepsilon'_C = (1 - f_{NT}) \log \varepsilon'_{PT} + f_{NT} \log \varepsilon'_{NT}, \quad (1)$$

such that f_{NT} denotes the volume fraction of the $NiTiO_3$ phase; ε'_{PT} and ε'_{NT} are the real part of permittivity at 1 MHz of $PbTiO_3$ and $NiTiO_3$ phases, respectively. Therefore, the increase in the nickel concentration leads to the situation where $\varepsilon'_C \sim \varepsilon'_{NT}$, corroborating the microstructural information on the composite nature of our ceramic samples, see Fig. S2 in Supplementary Data.

Table 1 summarizes the values for the phase transition temperature, T_C, obtained by measurements of Raman spectroscopy, differential scanning calorimetry and dielectric permittivity, for all compositions. By comparing these results, a good coherence among the transition temperature was detected, with very close T_C values obtained by three different techniques, proving that the synthesis

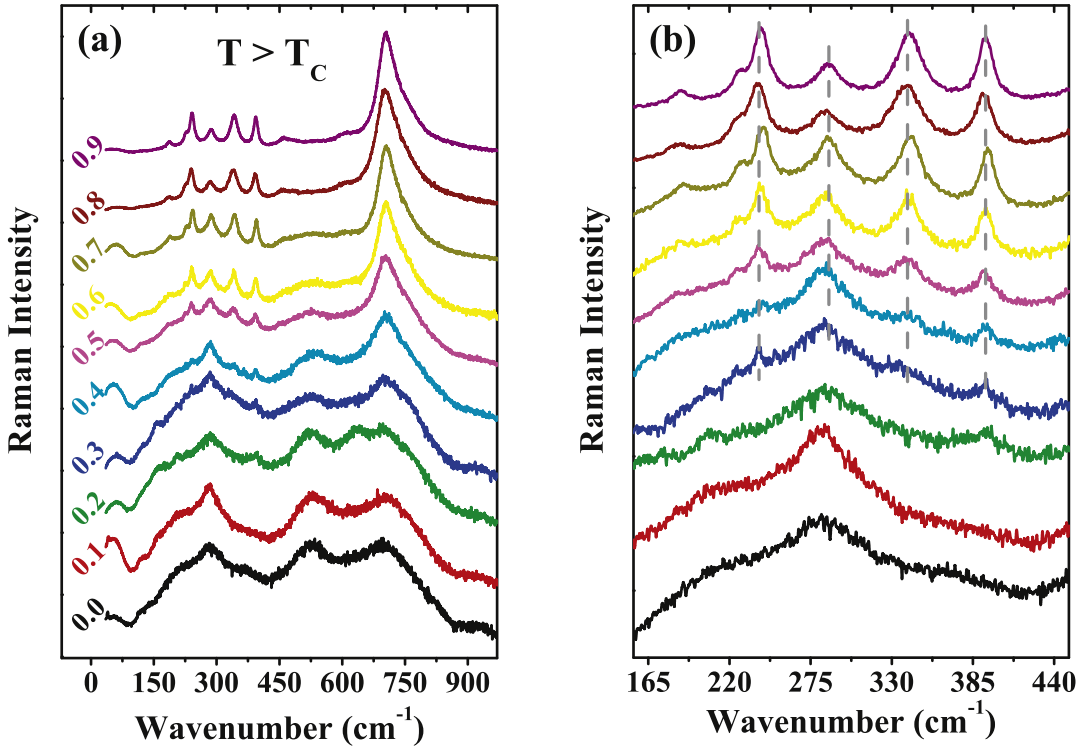

Fig. 3. (a) Raman spectra of $Ni_xPb_{1-x}TiO_3$ taken at temperatures above the $PbTiO_3$ tetragonal-ferroelectric to cubic-paraelectric phase transition (Curie temperature); (b) Wavenumber region in the range 165–440 cm^{-1}.

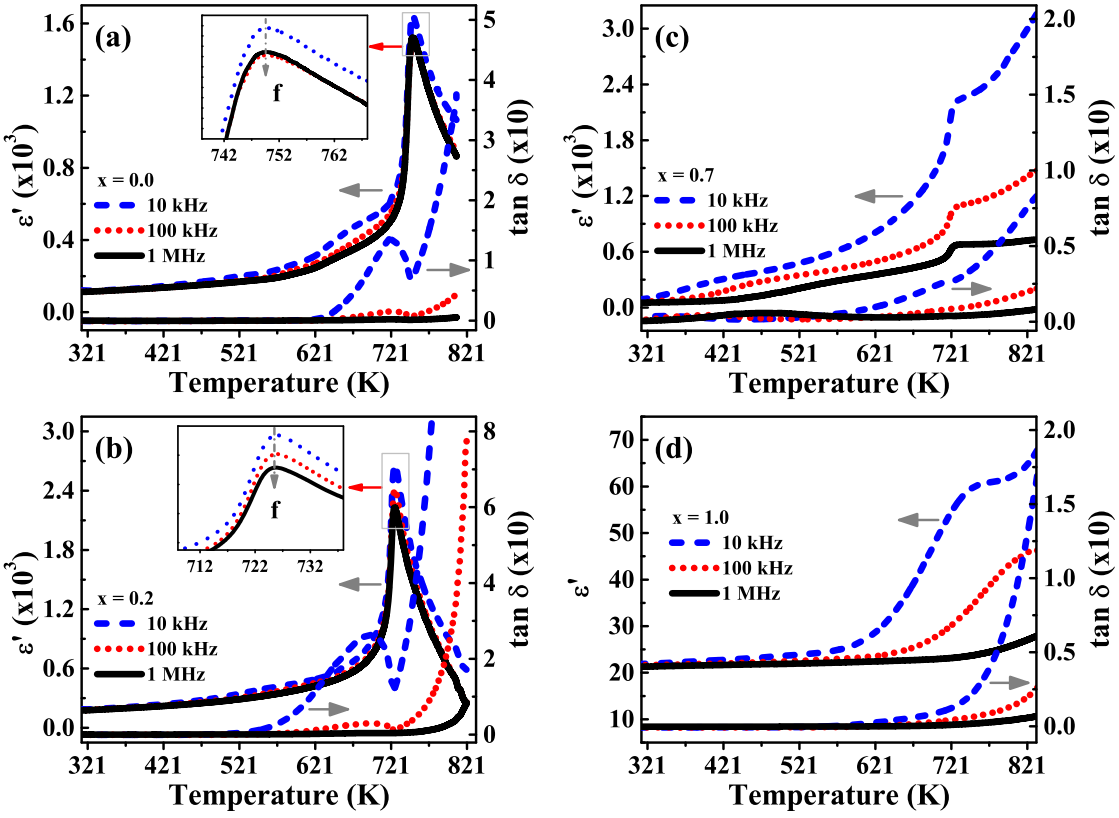

Fig. 4. Temperature dependence of the real part of the dielectric permittivity (ε′) and the dielectric loss (tan δ) of $Ni_xPb_{1-x}TiO_3$ for $x = 0.0$ (a); 0.2 (b); 0.7 (c) and 1.0 (d).

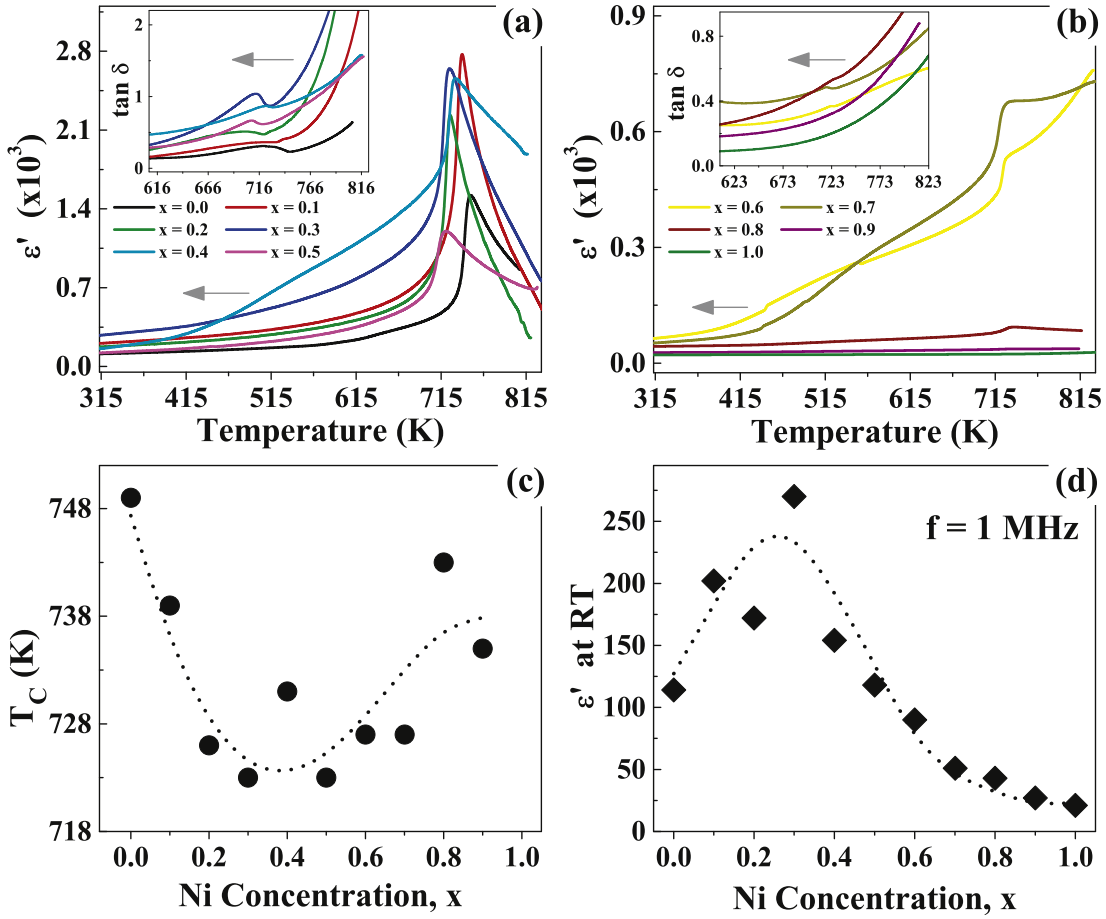

Fig. 5. Temperature dependence of the real part of the dielectric permittivity (ε′) and the dielectric loss (tan δ) at 1 MHz of $Ni_xPb_{1-x}TiO_3$ for $x = 0.0–0.5$ (a) and 0.6–1.00 (b). (c) T_C value dependence with the Ni content. (d) Dielectric constant collected at room temperature (1 MHz) dependence with the Ni content. Dashed lines are only guides to the eyes obtained after running average through the data.

Table 1
Values of T_C for NPT system derived from Raman, DSC and dielectric characterizations.

x: $Ni_xPb_{1-x}TiO_3$	Raman:T_c (K)	DSC:T_c (K)	Dielectric:T_c (K)
0.0	763	763	750
0.1	741	738	738
0.2	730	734	727
0.3	718	730	725
0.4	715	734	728
0.5	713	721	723
0.6	726	730	726
0.7	741	735	728
0.8	752	734	739
0.9	758	734	736

method is effective to tailor physical properties of the produces materials.

3.3. Magnetic properties

Fig. 6 shows the temperature dependence of the magnetic susceptibility (χ-H) of all samples, measured using FCC protocol at 50 Oe. The data taken from pure $PbTiO_3$ (PT) present a diamagnetic behavior, as expected. For the other compounds is observed an increase in the magnetic susceptibility value, proportional to the increase of the nickel concentration. The monotonic increase of the magnetic susceptibilities on cooling for samples with $x = 0.1$ and $x = 0.2$ indicate a paramagnetic behavior, which can be confirmed by the good fit of Curie's law equations with the experimental data, shown in fig Fig. 6 (b) [18]. The change from the diamagnetic behavior of pure PT to the paramagnetic behavior of these samples is an effect of the substitution of Pb by Ni in the solid solution formed in this compositional range [7]. FCC curves of samples in the interval $0.3 \leq x \leq 0.5$ (shown in details in Fig. 6 (c)) clearly do not follow the Curie's law in the whole temperature interval. The peaks appearing around 22 K are typical of antiferromagnetic transitions. They are consistent with that found in $NiTiO_3$ bulk, with Néel Temperature (T_N) of 23 K [19]. This transition is associated to the presence of $NiTiO_3$, revealed by our structural analyses. In the high concentration range, $0.6 \leq x \leq 1.0$, the amount of $NiTiO_3$ phase increases and its antiferromagnetic behavior stands out, implying an increasing in magnetic susceptibility. The increase of magnetic susceptibility at low temperature was explained by Yuvaraj et al. [20] and it was mainly related to grain size effect/structural defects. Although it is not possible to identify peaks in the Raman measurements referring to the $NiTiO_3$, the formation of this compound for concentrations above 0.3 was detected in magnetic measurements because the high sensitivity of the technique. No significant changes in the temperature of the antiferromagnetic transition of the samples were observed, confirming its relation with the presence of $NiTiO_3$.

Fig. 7 summarizes the results for the magnetization as a function of the magnetic field (M-H) at 300 K. It is possible to observe a

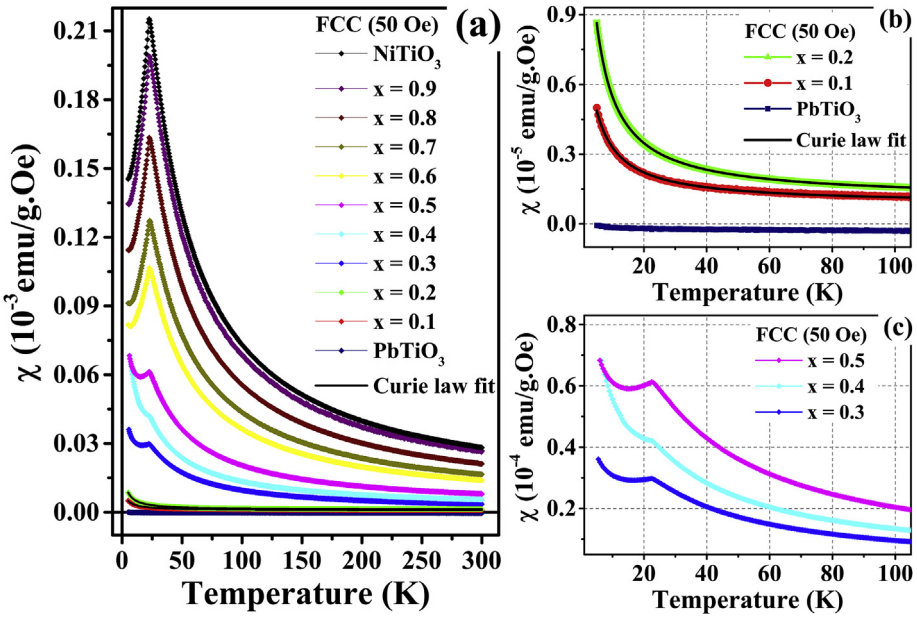

Fig. 6. Magnetic Susceptibility curves for the $Ni_xPb_{1-x}TiO_3$ at 50 Oe.

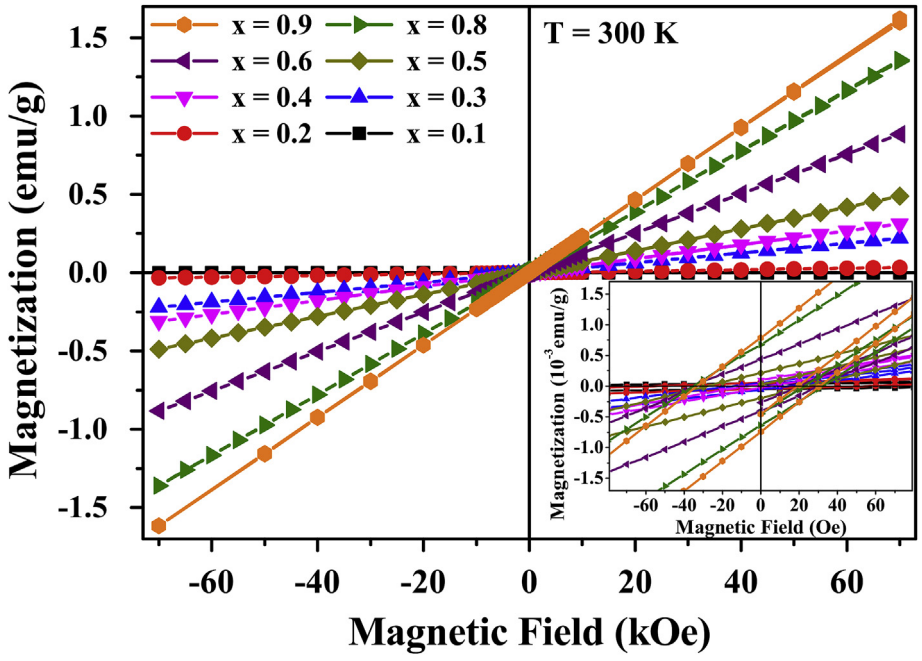

Fig. 7. Magnetization loop at 300 K for the $Ni_xPb_{1-x}TiO_3$.

typical paramagnetic behavior for Ni concentrations below 0.4 due to absence of remnant magnetization. A gradual increase in the remnant magnetization is observed for concentrations above 0.4, characterizing a weak ferromagnetic response. This ferromagnetic behavior is related to the formation of $NiTiO_3$, since no additional phases was identified. The ferromagnetic response in $NiTiO_3$ is due to the super exchange interaction between Ni^{2+} ions via oxygen atoms [20]. At these concentrations ($x > 0.5$), there is the formation of the composite in which NT is the magnetic phase while PT-like is the ferroelectric phase. Comparing the magnetization data with the Raman spectroscopy (see Fig. 8), it is possible to observe that for concentrations in which Ni substitution occurs ($x < 0.5$), a paramagnetic behavior is observed together with a decreasing of E(1TO) soft mode peak position (cm^{-1}), while for concentrations above 0.5 Ni a weak ferromagnetism takes place, accompanied by a recover tendency of E(1TO) soft mode peak position, that can be related to the composite formation.

4. Conclusions

A detailed study of structural, vibrational, dielectric and magnetic properties of $Ni_xPb_{1-x}TiO_3$ samples synthesized by solid state reaction method was performed by using X-ray diffraction, Raman scattering, dielectric permittivity, magnetic susceptibility and

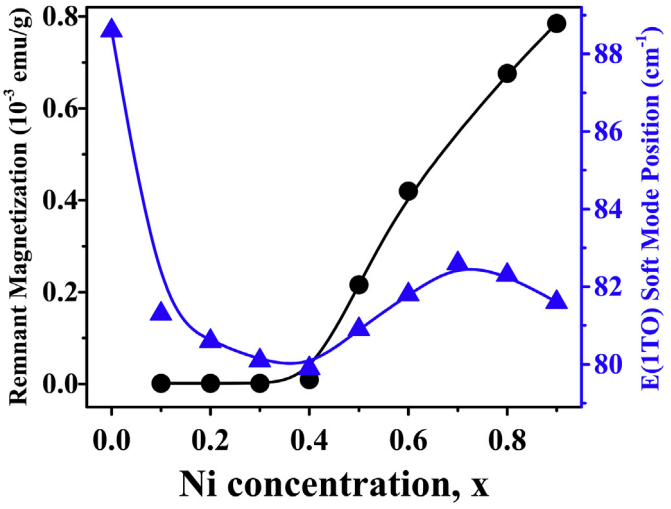

Fig. 8. Comparison between remanent magnetization (circle) and Raman soft-mode (triangle) for the $Ni_xPb_{1-x}TiO_3$. Solid lines are only guides to the eyes obtained after running average through the data.

magnetization loops. The XRD, Raman and magnetic susceptibility results showed the formation of solid solutions for x below 0.2, in which there is only ferroelectric order. For higher values of x there is preferentially the formation of a $PbTiO_3$ and $NiTiO_3$ composite, where there is also antiferromagnetic order. Therefore, the both dielectric and magnetic measurements exhibited the coexistence of the ferroelectric and antiferromagnetic orders for Ni concentrations where the material tends to form a composite, a very interesting result for magnetoelectric device application: By changing only the atomic substitution level, the material starts from ferroelectric and diamagnetic for $x = 0.0$, goes to ferroelectric and paraelectric for $0.0 < x < 0.2$, than to ferroelectric and antiferromagnetic for $0.2 < x < 0.90$ and finally non-ferroelectric and antiferromagnetic for $x = 1.0$. Moreover, the dielectric measurements corroborated the atomic substitution effect on the Curie temperature determined by the other techniques, in which there is a maximum of the real part of the dielectric constant for x values where there is a maximum of the $PbTiO_3$ unit cell volume contraction.

Acknowledgements

Financial support from Brazilian funding agencies CAPES, CNPq (proc. number 150936/2017-6), and FAPESP (grant. numbers 2013/07793-6 and 09/54082-2) is acknowledged.

Appendix A. Supplementary data

Supplementary data related to this article can be found at https://doi.org/10.1016/j.jallcom.2017.12.273.

References

[1] M. Sebastian, Dielectric Materials for Wireless Communication, first ed., Elsevier, 2008.
[2] A.S. Bhalla, R. Guo, R. Roy, The perovskite structure - a review of its role in ceramic science and technology, Mater. Res. Innovat. 4 (2000) 3–26.
[3] A.K. Kundu, Magnetic Perovskites: Synthesis, Structure and Physical Properties, Springer, India, 2016.
[4] G. Srinivasan, Magnetoelectric composites, Annu. Rev. Mater. Res. 40 (2010) 153–178.
[5] J.F. Scott, Applications of magnetoelectrics, J. Mater. Chem. 22 (2012) 4567.
[6] R. Roy, Multiple ion substitution in the perovskite lattice, J. Am. Ceram. Soc. 37 (1954) 581–588.
[7] R.C. da Costa, T.A. de Toledo, J.W.M. Espinosa, P.S. Pizani, Atomic substitution effects on the structural and vibrational properties of $Ni_xPb_{1-x}TiO_3$: X-ray diffraction and Raman scattering investigations, AIP Adv. 5 (2015) 77113.
[8] H.M. Rietveld, Line profiles of neutron powder-diffraction peaks for structure refinement, Acta Crystallogr. 22 (1967) 151–152.
[9] B.B. He, Two-dimensional X-Ray Diffraction, Wiley, 2011.
[10] E.C.S. Tavares, P.S. Pizani, J.A. Eiras, Short-range disorder in lanthanum-doped lead titanate ceramics probed by Raman scattering, Appl. Phys. Lett. 72 (1998) 897–899.
[11] D.A. Long, The Raman Effect: a Unified Treatment of the Theory of Raman Scattering by Molecules, John Wiley & Sons, West Sussex, England, 2002.
[12] A.R. West, D.C. Sinclair, N. Hirose, Characterization of electrical materials, especially ferroelectrics, by impedance spectroscopy, J. Electroceram. 1 (1997) 65–71.
[13] E. Barsoukov, J.R. Macdonald, Impedance Spectroscopy: Theory, Experiment, and Applications, second ed., Wiley, 2005.
[14] B.N. Sun, Y. Huang, D.A. Payne, Growth of large $PbTiO_3$ crystals by a self-flux technique, J. Cryst. Growth 128 (1993) 867–870.
[15] G. Burns, B.A. Scott, Lattice modes in ferroelectric perovskites: $PbTiO_3$, Phys. Rev. B 7 (1973) 3088–3101.
[16] M.I. Baraton, G. Busca, M.C. Prieto, G. Ricchiardi, V.S. Escribano, On the vibrational spectra and structure of $FeCrO_3$ and of the ilmenite-type compounds $CoTiO_3$ and $NiTiO_3$, J. Solid State Chem. 112 (1994) 9–14.
[17] A.V. Goncharenko, V.Z. Lozovski, E.F. Venger, Lichtenecker's equation: applicability and limitations, Optic Commun. 174 (2000) 19–32.
[18] F.H. Aragón, J.A.H. Coaquira, P. Hidalgo, S.L.M. Brito, D. Gouvêa, R.H.R. Castro, Structural and magnetic properties of pure and nickel doped SnO_2 nanoparticles, J. Phys. Condens. Matter 22 (2010) 496003.
[19] G.S. Heller, J.J. Stickler, S. Kern, A. Wold, Antiferromagnetism in $NiTiO_3$, J. Appl. Phys. 34 (1963) 1033–1034.
[20] S. Yuvaraj, V.D. Nithya, K.S. Fathima, C. Sanjeeviraja, G.K. Selvan, S. Arumugam, et al., Investigations on the temperature dependent electrical and magnetic properties of $NiTiO_3$ by molten salt synthesis, Mater. Res. Bull. 48 (2013) 1110–1116.